

**Langmuir-Blodgett deposition of multilayer PVDF thin films with NMP  
solvent**

*A thesis*

**Submitted in partial fulfillment of the requirement for the award of degree of**

**MASTER OF SCIENCE**

**in**

**PHYSICS**

**Submitted by**

**Kaveri Ajravat**

**(Roll No. 301604020)**



**Under the guidance of  
Dr. Loveleen K. Brar  
Assistant Professor**

**School of Physics and Materials Science  
Thapar Institute of Engineering and Technology  
Patiala- 147004  
June- 2018**

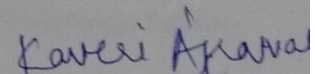
*Dedicated to*  
*My Family*  
*For their love and support*

## Certification

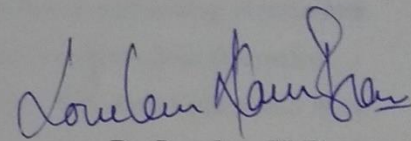
I hereby certify that this thesis entitled "Langmuir-Blodgett deposition of multilayer PVDF thin films with NMP solvent" in partial fulfillment for the requirements for the award of Degree of Master of Science in Physics submitted to School of Physics and Materials Science, Thapar Institute of Engineering and Technology, Patiala is an authentic record of my own work and is carried under the supervision of **Dr. Loveleen K. Brar**. The matter submitted via this thesis report has not been submitted for the award of any other degree to the best of our knowledge.

**Date:**

**Place:**

  
**Kaveri Agrawal**  
(301604020)

This is to certify that the above statement made by the candidate is correct and true to the best of my knowledge.



**Dr. Loveleen K. Brar**  
Assistant Professor  
Thapar Institute of Engineering and Technology  
Patiala- 147004

## Acknowledgement

First and foremost, I would like to express my sincere and deepest appreciation to my M.Sc. dissertation thesis supervisor, **Dr. Loveleen K. Brar** Assistant Professor, SPMS, Thapar Institute of Engineering and Technology, Patiala- 147004, India for her valuable discussions and suggestions, guidance, strong motivation, encouragement and inspiration throughout my M.Sc. dissertation thesis journey.

I also express my heartiest gratitude to **Dr. Manoj Kumar Sharma**, Head and Professor, School of Physics and Materials Science of Thapar Institute of Engineering and Technology, Patiala-147004, India for his support throughout the period.

I would like to express my deepest gratitude to **Dr. Puneet Sharma** and **Dr. B.N. Chudasama** for letting me avail the facilities in their respective laboratories and for their valuable support during this period.

A special thanks to **Ms. Raveena Choudhary** for her valuable guidance in learning the technique.

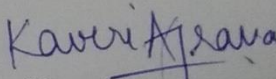
I am thankful to **Ms. Isha Kalra** and **Mr. Ajit Seth** for helping me in performing experiments and analyzing the data and for being a constant support and companion throughout this period.

I would like to express my deepest gratitude to my beloved parents **Mr. Anil Kumar** and **Mrs. Sudesh Kumari** and elder brother **Mr. Sahil Ajravat**, who has always believed in me, and endured with me during difficult times. I am thankful to my cousin sister **Mrs. Shimpi Kathuria** and my cousin brother **Mr. Kartik Ajravat** and their family for their valuable support.

I would like to express my love to my best friends, **Mr. Sameer Saluja**, **Ms. Gaganjot Kaur**, **Ms. Jaspreet Kaur**, and **Ms. Harsimranpreet kaur** who inspire me every day to be strong and keep me going with their smile and love.

Last but not least, deepest thanks to all the friends who have always been with me.

Date:

  
Kaveri Ajrayat

## Abstract

Polyvinylidene Fluoride (PVDF) is a promising homopolymer in view of its wide range of applications. PVDF thin films have been utilized in energy gathering applications, manufacturing of sensors, biological applications etc. This is due to the extraordinary behavior shown in the  $\beta$ -phase crystal structure of PVDF thin films exhibiting pyroelectric, ferroelectric and piezoelectric properties. The thin films of PVDF are prepared by Langmuir-Blodgett technique which provides a unique layer by layer control on the film fabrication parameters which is important from the application point of view. In the present work, the PVDF thin films are prepared by Langmuir-Blodgett deposition method with NMP solvent. To obtain good transfer characteristics the PVDF Langmuir layers were characterized for different spreading solution concentration and compression rates at 18 °C. The isotherm, hysteresis and barrier oscillation experiments show that the most stable PVDF films were obtained for spreading solution molarity of 0.0936 mol/l and 20 mm/min compression rate. These trough parameters were used for the deposition of the PVDF LB films. The role of spreading solution molarity in sharply determining the MMA and elasticity of the monolayer indicates that the initial interaction of the PVDF with the solvent (NMP) plays an important role in determining the spreading solution characteristics. A good TR is obtained for the first upstroke at 2 mm/min speed for the glass substrate. But downstrokes result in dissolution of the deposited films and also TR is reduced in the subsequent upstrokes. This indicates that Z-type nature of the PVDF LB films which is getting disrupted due to the partial dissolution of PVDF into water during downstrokes. To avoid this every single layer deposition was followed by sub-phase change. Multilayer transparent films of PVDF were synthesized by deposition of 1, 3 and 8 layers on the followed by drying and annealing. The topographic analysis of the final films shows the emergence of few large crystallites which makes the films rough.

# Contents

<b>S. No.</b>	<b>Title</b>	<b>Page No.</b>
	<b>List of figures</b>	Vii
	<b>List of tables</b>	Viii
<b>Chapter 1</b>	<b>Introduction to Polyvinylidene Fluoride (PVDF) thin films</b>	
1.1	Thin films	1
1.2	Polyvinylidene Fluoride (PVDF)	2
1.3	PVDF thin films	4
1.4	Properties of PVDF thin films	5
1.5	Applications of PVDF thin films	5
1.6	References	5
<b>Chapter 2</b>	<b>Literature Survey</b>	
2.1	Langmuir-Blodgett Deposition method for amphiphilic molecules	6
2.2	Role of barrier oscillation in determining deposition parameters	6
2.3	Synthesis of PVDF thin films with various methods	7
2.4	Synthesis of PVDF thin films by Langmuir trough	8
2.5	References	9
<b>Chapter 3</b>	<b>Materials and Methods</b>	
3.1	Materials	10
3.2	Experimental method	11
3.3	Langmuir-Blodgett Method	13
3.3.1	Assembly of Langmuir-Blodgett technique	13
3.3.2	Fabrication and Deposition of Langmuir monolayer	14
3.3.3	Types of deposition	15
3.3.4	Transfer ratio	16
3.4	Characterization techniques	16
3.4.1	Surface pressure-Area Isotherm	16
3.4.2	Hysteresis	17
3.4.3	Barrier Oscillation	18
3.4.4	Atomic Force Microscopy (AFM)	18

3.5	References	19
<b>Chapter 4</b>	<b>Results and Discussions</b>	
4.1	Surface Pressure-Area ( $\Pi$ -A) Isotherms	20
4.1.1	Effect of molarity of spreading solution	20
4.1.2	Effect of Barrier Speed	21
4.2	Hysteresis analysis of $\Pi$ -A isotherms	23
4.3	Barrier Oscillation	25
4.3.1	Effect of various frequencies on barrier oscillation	25
4.3.2	Effect of different molarities of PVDF with barrier oscillation	27
4.3.3	Effect of barrier speed change with barrier oscillation	29
4.4	Deposition of PVDF Langmuir-Blodgett thin films	32
4.5	Topography Analysis	33
4.6	References	34
<b>Chapter 5</b>	<b>Conclusion and future scope</b>	
5.1	Conclusion	35
5.2	Future scope	35

## List of Figures

<b>Figure No.</b>	<b>Description</b>	<b>Page No.</b>
1.1	Schematic of a thin film on a substrate	1
1.2	Structure of polyvinylidene fluoride (PVDF)	2
1.3	(a) trans (T) and gauche (G) chain formations in PVDF, (b) various conformational phases of the PVDF crystal	3-4
3.1	Structure of NMP	10
3.2	PVDF monolayer spread on the water subphase	11
3.3	Amphiphilic molecule accordant for Langmuir-Blodgett method	13
3.4	Assembly of Langmuir-Blodgett method	14
3.5	Types of deposition	15
3.6	Surface pressure-area isotherm	16
3.7	Hysteresis curve for Langmuir monolayer	17
3.8	(a) Schematic of Atomic Force Microscopy, (b) Laboratory view of AFM	19
4.1	(a) $\Pi$ -A isotherms for different molarities of PVDF dissolved in NMP on DI water as subphase at temperature 18°C, spreading solution volume of 50 $\mu$ l and barrier speed of 30 mm/min., and (b) variation of mean molecular area of liquid and solid phase (MMA) and elasticity with different molarities	20
4.2	(a) $\Pi$ -A isotherms for different barrier speed of 0.0936 mol/l PVDF spreading solution at temperature 18°C and spreading solution volume of 50 $\mu$ l and (b) variation of mean molecular area of liquid and solid phase (MMA) and elasticity with different barrier speeds	22
4.3	Hysteresis curves showing variation of surface pressure with MMA for barrier speed 30 mm/min at temperature 18°C	23
4.4	(a) Variation of liquid phase and solid phase with cycle no. for barrier speed (10, 20 and 30) mm/min, (b) variation of static elasticity with cycle number for different barrier	24
4.5	Surface pressure variation with time for different frequencies at temperature 18°C and 20 mm/min barrier speed	26
4.6	Graph showing the variation for $ G $ , $G'$ , $G''$ with various frequencies	27
4.7	Variation of surface pressure with time for different molarities at temperature 18°C and 20 mm/min barrier speed with frequency for barrier oscillation at 30 mHz	28
4.8	Graph showing the variation of static elasticity, $ G $ , $G'$ , $G''$ with molarity change	29
4.9	Variation of surface pressure with time for barrier speed change	30

	at temperature 18°C and barrier speed of 20 mm/min with frequency for barrier oscillation at 30 mHz	
4.10	Graph showing variation of static elasticity, $ G $ , $G'$ , $G''$ with different barrier speeds	31
4.11	(a), (b), (c), and (d) graphs shows the variation of Transfer ratio with layer number at temperature 18 °C with barrier speed of 20 mm/min. and spreading 100 $\mu$ l of 0.0936 mol/l PVDF spreading solution	32
4.12	AFM images of PVDF Langmuir-Blodgett films on glass substrate. 15 $\mu$ m $\times$ 15 $\mu$ m AFM images of a) 1 layer c) 3 layers d) 8 layer film. b) 3 $\mu$ m $\times$ 3 $\mu$ m, image of 1 layer film in the smoother region	34

### List of Tables

Table No.	Description	Page No.
1.1	Types of materials	1
3.1	PVDF samples prepared	13
4.1	Values of mean molecular area for liquid phase ( $MMA_L$ ) and solid phase ( $MMA_S$ ) with static elasticity of solid phase for different molarities of PVDF in the spreading	21
4.2	Values of mean molecular area of liquid phase ( $MMA_L$ ) and solid phase ( $MMA_S$ ) and static elasticity of solid phase for different barrier speed for compression	22
4.3	For barrier speeds (10, 20 and 30) mm/min values of mean molecular area of liquid phase ( $MMA_L$ ) and solid phase ( $MMA_S$ )	24
4.4	Values of static elasticity of solid phase for consecutive cycles of compression	24
4.5	Values of $ G $ , $G'$ , $G''$ for various frequencies of barrier oscillation	27
4.6	Values of $ G $ , $G'$ , $G''$ for different molarities of PVDF of barrier oscillation.	28
4.7	Values of $ G $ , $G'$ , $G''$ for different barrier speeds of compression	30
4.8	Roughness analysis of the AFM images	33

### Introduction to Polyvinylidene Fluoride (PVDF) thin films

#### 1.1 Thin films

Nanomaterials arise because of confinement of the extent of the materials  $< 100$  nm (nearly). In nano regime, one encounters three types of materials: zero-dimensional, one-dimensional, two-dimensional (Table 1.1). The type of nano-material formed is defined by the number of dimensions or axes which undergoes confinement in space.

**Table 1.1:** Types of materials

Material	Confinement of axes	Examples
Bulk (3-D)	0	Wood
2-D	1	Thin films
1-D	2	Nano wire
0-D	3	Quantum dots

The thin films are the materials which are spread in only two dimensions i.e. x and y axis, in the form of a thin plate or film in nano dimensions. The films which have their thickness in the scale of nano meters are known as thin films [1]. Figure 1.1 shows the schematic of a thin film on a substrate.

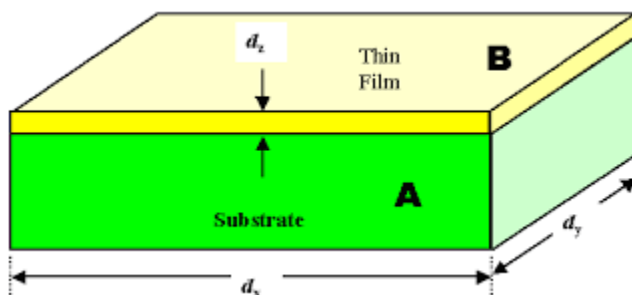


**Figure 1.1:** Schematic of a thin film on a substrate [2].

In thin films, the organic or inorganic material of nm thickness is deposited on a solid substrate. The deposited film on the substrate is then studied for its properties. For good thin film deposition, good adhesion between the material to be deposited and the substrate should be there so that the material sticks to the substrate properly. The most natural system of thin film observed in nature is oil in water thin film.

Properties observed in thin films are as follows:

- Higher critical yield strength as compared to the bulk forms.

- Thin films are more transparent as compared to their bulk counterparts.
- Thin films can bear a lot of stress without collapsing.
- Higher electrical collapse field strength which allows the thin films to be operated on voltages ~10V.
- Higher critical current density as compared to the bulk counterpart [2].

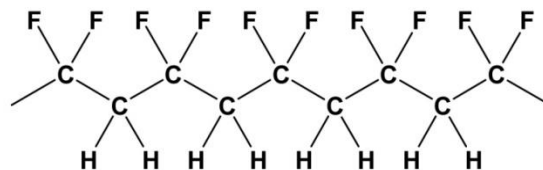
In the mid 90's the thin films were used for optical, electronic, mechanical and protective applications. With the advancement of technology, thin films have been used in various fields and in huge number of applications. In the semiconductor industry, thin films are widely used for the fabrication of miniaturized memory chips with improvement in the element density from 50 to 5000 elements per mm sq. units over the years [1].

A thin film has numerous potential applications which have helped the mankind to grow more in the field of technology. Some of the applications are listed below:

- In the field of optics, thin films have been used in making of anti-reflection coatings on lenses, coatings for decoration etc.
- In the field of magnetics, it has been used to manufacture hard discs.
- Thin films are used to provide resistance against corrosion.
- It has been utilized in manufacturing of insulating and conducting films.
- Thin films are used to manufacture solar cells.
- It has been used in mechanical industry, to provide resistance against abrasion.
- Thin films are used to fabricate semiconductor devices [2].

## 1.2 Polyvinylidene Fluoride (PVDF)

Polyvinylidene Fluoride is a polymer derived from a free radical polymerization of 1, 1-difluoroethene. The homopolymer obtained is a thermosetting polymer i.e. it is resistant to high temperatures and can retain its shape permanently once formed. It is highly inert in nature. The structure of PVDF is as shown in figure 1.2 below:

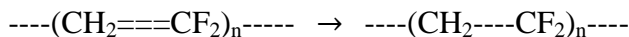


Polyvinylidene fluoride (PVDF)

**Figure 1.2:** Structure of Polyvinylidene Fluoride (PVDF).

---

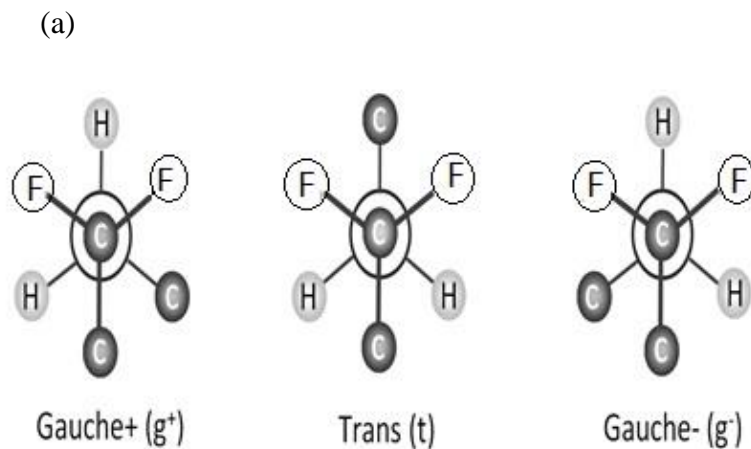
The polymerization of vinylidene fluoride to form polyvinylidene fluoride happens as follows:



PVDF has been used for a variety of applications due to its various properties and hence is widely used. Its properties are as follows:

- Resistant to creep and fatigue.
- High dielectric constant.
- High dipole moment (2.1D).
- Good stability towards radiation (UV radiation, thermal radiation).
- Glass transition temperature  $-35^\circ\text{C}$ .
- Stable in temperature range of  $-20^\circ\text{C}$  to  $130^\circ\text{C}$  [3].

PVDF polymer has various orientations in space due to which it exists in five different crystalline phases namely  $\alpha$ -phase,  $\beta$ -phase,  $\gamma$ -phase,  $\delta$ -phase and  $\epsilon$ -phase when its molecular chains are stretched in space. Among these five crystalline phases, the phases which are mostly studied are  $\alpha$ -phase,  $\beta$ -phase,  $\gamma$ -phase. The  $\alpha$ -phase is non-polar while the  $\beta$ -phase and the  $\gamma$ -phase are polar in nature. The different phases are the result of different conformations which are formed when carbon, hydrogen and fluorine atoms are placed in different orientations with respect to each other in space. The trans (T) and gauche (G) chains form  $\alpha$ -phase as (TGTG'),  $\beta$ -phase as (T<sub>4</sub>) and  $\gamma$ -phase as (T<sub>3</sub>GT<sub>3</sub>G'). The gauche linkages are those linkages in which the molecular bonds are aligned at  $60^\circ$  with respect to each other in space due to torsional strain [4]. The trans and gauche structures for PVDF and the three crystal phases of PVDF is as shown in figure 1.3 (a) and (b) below:



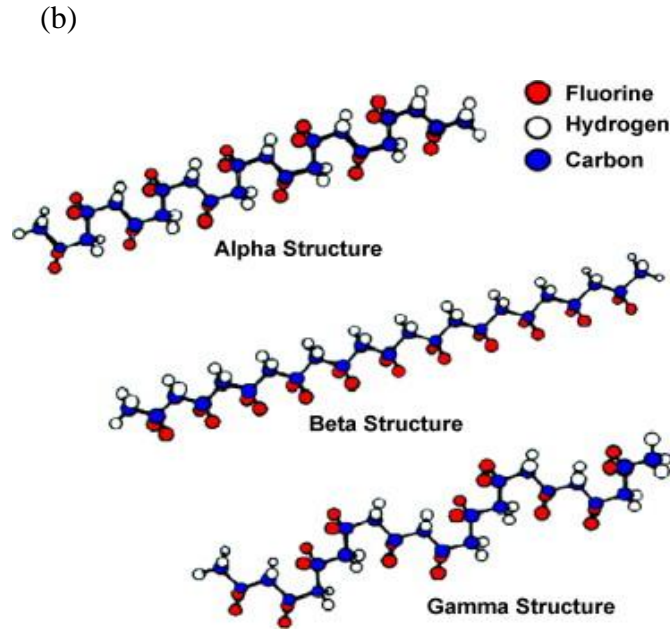


**Figure 1.3:** (a) trans (T) and gauche (G) chain formations in PVDF, (b) various conformational phases of the PVDF crystal [5].

The  $\alpha$ -phase is achieved by melting and is then crystallized normally. The  $\beta$ -phase in PVDF is acquired from the  $\alpha$ -phase by cold drawing, by high pressure annealing or by high electrical field poling. The resulting  $\beta$ -phase is sometimes less oriented in 3-D due to low processing temperature and therefore, to obtain highly oriented  $\beta$ -phase, the process temperature should be high [7]. PVDF homopolymer shows excellent ferroelectric and pyroelectric properties when stretched under force in space. Due to existence of good ferroelectric properties, PVDF has been synthesized in numerous applications [4].

### 1.3 PVDF thin films

Polyvinylidene Fluoride (PVDF) thin films can be synthesized by various methods such as melt casting, spin coating, solvent casting etc. PVDF is an amphiphilic molecule that contains hydrophilic part and hydrophobic part. Due to its amphiphilic nature, the thin films of PVDF can be made by Langmuir-Blodgett method by dissolving it in suitable solvent. The different phases formed in the thin films can be utilized in various ways. The formation of  $\beta$ -phase in PVDF thin films is achieved by annealing the thin film which transforms PVDF from  $\alpha$ -phase to the  $\beta$ -phase. The properties of PVDF thin films can be altered with formation of different phases. This piezoelectric and ferroelectric behavior of PVDF thin films have been used for numerous applications [6].

---

## 1.4 Properties of PVDF thin films

Properties of PVDF thin films are listed below:

- Piezoelectric coefficient: (-49.4pm/V).
- Remanent polarization: (69.5mC<sup>2</sup>/m).
- Heating rate determines the pyroelectric coefficient.
- High dielectric constant.
- Highly stable  $\beta$ -phase which shows good ferroelectric properties [6].

## 1.5 Applications of PVDF thin films

PVDF thin films can be utilized in number of useful applications due to its promising properties such as good ferroelectric, pyroelectric and piezoelectric behavior. Some of the applications are listed as:

- The piezoelectric property has been used in the manufacturing of various sensors.
- The ferroelectric property has been utilized in processing of non-volatile memory chips and devices due to high remanent polarization.
- It can be widely used as magnetoelectric material with high coupling constant.
- PVDF thin films along with other elements as matrix can used in the energy gathering applications due to its pyroelectric and piezoelectric properties.
- PVDF thin films are used in various biological purposes such as tissue engineering.
- It has been helpful in developing the 3-dimensional structure transfiguration [7].

## 1.6 References

1. A. Wagendristel and Yuming Wang, “An introduction to Physics and Technology of thin films”, World scientific publishing Co. Pte. Ltd., QC176.83.W34 (1994).
2. Prof. Dr. Helmut Föll, Semiconductor Technology Script, Faculty of Engineering, University of Keil.
3. Zhang et al., *Encyclopedia of smart materials*, vol. 1-2 (2002) 807-825.
4. Lolla dinesh et al., *Materials*, (2016-08-09) 9(8):671.
5. Dali Yang et al., *Journal of membrane science*, 409-410 (2012) 302-317.
6. Prevedouros K et al., *Environ sci technol.*, (Jan 2006) 40(1):32-44.
7. Liuxia Ruan et al., *Polymers*, 10(3) (2018) 228.

**Overview**

In the present chapter, the literature survey based on Langmuir-Blodgett deposition method for amphiphilic molecules, role of barrier oscillation in determining the deposition parameters, synthesis of PVDF thin films with various methods and synthesis of PVDF Langmuir-Blodgett films have been discussed.

**2.1 Langmuir-Blodgett deposition method for amphiphilic molecules**

**R.H. Tredgold (1987) [1]:** Langmuir films are formed with the amphiphilic molecules which contains hydrophilic and hydrophobic part. Generally polymers containing the functional groups which are capable hydrogen bonding are used to form monolayers with this method. The monolayer formed is deposited on the glass substrate and the surface pressure-area isotherm is recorded. The monolayer deposited can be of X, Y, Z type depending upon the substrate. Various characterization techniques are used to study the properties of thin films.

**Osvaldo N. et al. (1992) [2]:** Over the years, Langmuir-Blodgett method, for deposition of monolayers has gained significance in the field of materials science. LB method is used for the deposition of single or multiple monolayers and is very efficient method in a way for monitoring the thickness of thin films. It measures pressure of the monolayer and give the surface pressure-area isotherms which helps to study the characteristics of the monolayer formed.

**2.2 Role of Barrier Oscillation in determining the deposition parameters**

**Hani Hilles et al. (2006) [3]:** The material molecules are spread on Langmuir trough and is compressed with the barriers and stress in the monolayer occurs. The barrier oscillation gives various stress-strain plots. The Fourier Transform (FT) analysis of the waves obtained from barrier oscillation shows that the experimental and theoretical amplitude coincide to some extent and amplitude of stress was recorded to be 8 %.

**Xiaolin Li. et al. (2008) [4]:** Graphene oxide thin films were prepared from Langmuir-Blodgett deposition. The deposited films were dried at 350 °C. The films were transferred one at a time and the substrate was deposited with three monolayers of graphene sheet (GS). The resistance of sheet was observed as 8 K $\Omega$  at a transparency of 80 % which is in agreement with the natural

---

GS. This was a successful experiment and had a great potential in using GS in various applications in the field of electronics.

**D.Y. Zhang et al. (2010) [5]:** The Barrier Oscillation method in the Langmuir-Blodgett experiments, is used for the study of shear and compression modulus of the Langmuir monolayers. The Wilhelmy plate is kept parallel and perpendicular to the barriers. There was an increase in the amplitude and phase of the shear and compression modulus with increment in strain for the compression layers. In the layers of deposition, the curves are not sine waves for low value of amplitude.

### **2.3 Synthesis of PVDF thin films with various methods**

**K.L. Choy et al. (2000) [6]:** Electrostatic spray-assisted vapour deposition method was used to prepare PVDF thin films. A high voltage or corona discharge is involved in the preparation of PVDF thin films dissolved in DMF solvent. Due to this, mechanical stretching occurs and a highly oriented  $\beta$  phase crystals are formed as thin films on the substrate. For  $\beta$  phase absorption band was observed at 530 and 1280  $\text{cm}^{-1}$ .

**A Salimi et al. (2004) [7]:** Solution film casting was done to prepare PVDF thin films dissolved in N,N dimethylacetamide (DMAc) and cyclohexanone. PVDF when dissolved with cyclohexanone produces  $\alpha$  phase crystals due to low polarity changes while PVDF when dissolved with DMAc produces rich  $\beta$  phase crystals due to high intermolecular and dipole interactions. The piezoelectric constant of the  $\beta$  phase PVDF thin films comes out to be of the range of (21-24) pC/N for a temperature range of (60-120)  $^{\circ}\text{C}$ .

**Xujiang He et al. (2006) [8]:** PVDF thin films were deposited by spin coating method by dissolving PVDF in a volatile solvent Dimethylformamide (DMF). The  $\alpha$ ,  $\beta$  and  $\gamma$  phase were obtained with this spin coating method depending upon the condition that whether  $\text{Mg}(\text{NO}_3)_2 \cdot 6\text{H}_2\text{O}$  was added to the dissolved solution of PVDF or not. The ferroelectric rich  $\beta$ -phase was obtained when mixed with  $\text{Mg}(\text{NO}_3)_2 \cdot 6\text{H}_2\text{O}$  due to strong intermolecular interactions and dipole interactions between PVDF in DMF and  $\text{Mg}(\text{NO}_3)_2 \cdot 6\text{H}_2\text{O}$  as is evidenced from the wide absorption band of 2923 to 3702  $\text{cm}^{-1}$  from FTIR analysis. Also, the remanent polarization was observed as 69.5  $\text{mC/m}^2$ .

**Vikram S Yadav et al. (2010) [9]:** PVDF thin films were prepared by film casting by dissolving PVDF in a suitable volatile solvent such as dimethyl acetate. For dielectric measurements, the PVDF thin film was sandwiched between Al electrodes. It was observed that the dielectric loss

---

decreases with increasing frequency. For a certain temperature, the dielectric constant increases and then decreases. These results are observed due to the dipole interactions in the PVDF thin films.

**Mengyuan Li. et al. (2013) [10]:** The PVDF thin films were prepared by wire-bar (Meyer rod) coating. The films were produced at a relative humidity of (0-60) % and at raised substrate temperature till 120 °C which was successful in the formation of smooth films with reduced roughness. The roughness characterized by SEM and AFM was observed as 1 nm for a 10 nm width of PVDF thin film and hence was smooth enough to be used as a potential tool in making of devices in microelectronics.

## 2.4 Synthesis of PVDF thin films by Langmuir trough

**V.V. Kochervinskii et al. (2010) [11]:** The  $\beta$  phase of PVDF is formed with PVDF homopolymer with deposition on a solid substrate by Langmuir Schaefer method at low temperature and leads to the zig-zag type structure of the  $-(\text{CH-CF})-$  bonds. This leads to the TGTG type of conformation. While at the high temperature  $\gamma$  phase is formed of PVDF which has a chair type structure of  $-(\text{CH-CF})-$  bonds and leads to  $\text{T}_3\text{GT}_3\text{G}$  conformation. The  $\beta$  phase has a good dipole moment and has a very good piezoelectric and pyroelectric properties which make it an important polymer in the nanotechnology.

**Shuting Chen et al. (2012) [12]:** The PVDF homopolymer is deposited on the Si substrate through Langmuir Schaefer deposition with width of 29 nm for 20 layers. The XRD peak for  $\beta$  phase was at  $20.8^\circ$  which confirmed the formation of  $\beta$  phase crystals on the deposited thin film. Hydrogen bonding present between the PVDF and subphase is supported by the absorption band of  $3235\text{ cm}^{-1}$  from FTIR studies. The piezoelectric coefficient was observed to be  $-49.4\text{ pm/V}$ .

**Huie Zhu et al. (2014) [13]:** PVDF nanofilms show remarkable features such as remanent polarization which is extensively used in the molecular electronics. The extrinsic switching properties were studied of the PVDF thin films deposited by Langmuir-Blodgett deposition. Various PVDF thin films were made of variable layers and the one best recorded and showed excellent feature of ferroelectric behavior was at 81 nm. Each layer was 5 nm in width and the properties became less valueable with the films in width greater than 100 nm.

**Subrata Maji et al. (2015) [14]:** PVDF  $\beta$  phase shows good ferroelectric and piezoelectric properties. The 30 monolayers deposited of PVDF by Langmuir Schaefer method is quite stable and has achieved  $\sim 99\%$  proportion of  $\beta$  phase and is utilized in various applications The  $(\text{CH}_2-$

---

CF<sub>2</sub>) units in the PVDF is responsible for the dipole moment with respect to the subphase as the number of monolayer increases. This results in a good  $\beta$  phase which is thermodynamically stable and can be utilized in many electronics based applications.

**Chandan Kumar et al. (2017) [15]:** PVDF thin films were deposited on the Si substrate by horizontal Langmuir Schaefer deposition, using various solvents i.e. polar as well as non-polar solvents like Dimethylsulfoxide (DMSO), Methyl ethyl ketone (MEK) etc. Different solvents act as good and swelling solvents and behave differently when PVDF is dissolved in them. The Elasticity values, surface potential values shows the formation of the  $\alpha$ ,  $\beta$  phases of PVDF. It is observed that usually polar solvents leads to the formation of  $\beta$  phase and the non-polar solvents leads to the formation of  $\alpha$  phase.

## 2.5 References

1. R.H. Tredgold, *Rep. Prog. Phys.*, 15 (1987) 1609-1656.
2. Osvaldo N. et al., *Brazilian Journal of Physics*, 22(2) (1992) 60-68.
3. Hani Hilles et al., *Advances in colloid and interface science*, 122 (2006) 67-77.
4. Xiaolin Li. et al., *Nature nanotechnology*, 3 (2008) 538-542.
5. D.Y. Zhang et al., *Eur. Phys. J. E*, 31 (2010) 125-134.
6. K.L. Choy et al., *Thin Solid Films*, 372 (2000) 6-9.
7. A Salimi et al., *Wiley Interscience*, (2004) 3487-3495.
8. Xujiang He et al., *Appl. Phys. Lett.*, 89 (2006) 112909.
9. Vikram S Yadav et al., *International MultiConference of Engineers and Computer Scientists (IMECS)*, 3 (2010).
10. Mengyuan Li. et al., *J. Mater. Chem. C*, 1(46) (2013) 7695-7768.
11. V.V. Kochervinskii et al., *Polymer Sci Series A*, 52(1) (2010) 40-48.
12. Shuting Chen et al., *Polymer*, 53 (2012) 1404-1408.
13. Huie Zhu et al., *J. Mater. Chem. C*, 2 (2014) 6727-6731.
14. Subrata Maji et al., *Phys. Chem. Chem. Phys.*, 17 (2015) 8159-8165.
15. Chandan Kumar et al., *European Polymer Journal*, 86 (2017) 132-142.

---

## Chapter 3

### Materials and Methods

#### Overview

In this chapter, materials and methods which have been used for the synthesis and characterization of PVDF Langmuir-Blodgett thin films have been discussed.

#### 3.1 Materials

Following materials are required for the preparation of PVDF thin films:

1. **Polyvinylidene fluoride (PVDF):** It is a homopolymer obtained by free radical polymerization. It is used for forming the monolayer on the subphase. It is procured from Alfa Aesar with 98% purity.
2. **N-methyl-2-pyrrolidone:** The solvent used for the dissolution of PVDF is N-methyl-2-pyrrolidone also called as NMP. Figure 3.1 shows the structure of NMP.

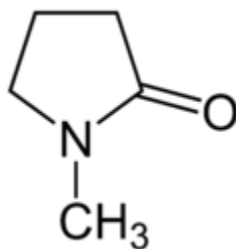


**Figure 3.1:** Structure of NMP.

It is an organic compound which contains ketone as a functional group. It is an aprotic solvent i.e. the hydrogen bonds are not detached easily from it. The NMP has Hansen solubility parameter (HSP) for polar nature of  $12.3 \text{ MPa}^{1/2}$ . This value indicates the affinity of the PVDF with solvent. NMP is a good solvent w.r.t to the dissolution of the PVDF in the solvent as is evident from the HSP value. NMP shows a good dipole moment of 12.26 D which makes it a good bonding agent with the PVDF [1]. It has good dissolution properties and hence mixes very well with the PVDF and evaporates easily. It is procured from Loba Chemie Pvt. Ltd. with purity of 98%.

3. **Acetone:** The cleaning of the microsyringe, glass slides, Wilhelmy plate etc. is done with acetone. It was purchased from RANKEM with purity >99%.
4. **Methanol:** The cleaning of trough and barriers is done with methanol and is obtained from SDFCL (HPLC grade).
5. **Propanol:** The cleaning of trough and barriers is followed by propanol after it is done with methanol. It was a product of fisher scientific with purity of (=99.7%).

- 
- Type-3 (Ultra-pure water):** The type-3 water is deionized water and is used in cleaning of trough, barriers and glass slides. It is also used as a subphase and was a product of Milipore ultrapure water systems with resistivity of 18.2 M $\Omega$ .
  - Glass slides:** The deposition of the LB thin films was done on the borosil<sup>TM</sup> glass slides cut in size of 26mm  $\times$  26mm  $\times$  1mm.

### 3.2 Experimental method

The following steps were used while performing the experiment:

- Trough and barrier cleaning:** The trough and barriers are cleaned properly prior to the addition of the water subphase with methanol, propanol, type-2 (distilled water) and type-3 (ultra-pure water) respectively two to three times.
- Subphase preparation:** The fresh subphase is type-3 ultra-pure water or deionized water at 18.2 M $\Omega$  resistivity.
- Spreading solution preparation:** The Polyvinylidene Fluoride (PVDF) in predetermined concentration is mixed with NMP and ultrasonicated for 5 minutes at room temperature to prepare the spreading solution. Different molarities of PVDF used are: 0.0312 mol/l, 0.0468 mol/l, 0.0624 mol/l, 0.0936 mol/l, 0.1249 mol/l, 0.1874 mol/l. This solution is used to prepare the Langmuir monolayers of PVDF on water.
- Langmuir-monolayer formation and isotherm characterization:** 50  $\mu$ l of the PVDF solution is spread dropwise on the water surface with help of microliter syringe. Half an hour is allowed for evaporation of the NMP. Figure 3.2 shows PVDF monolayer spread on the water subphase.

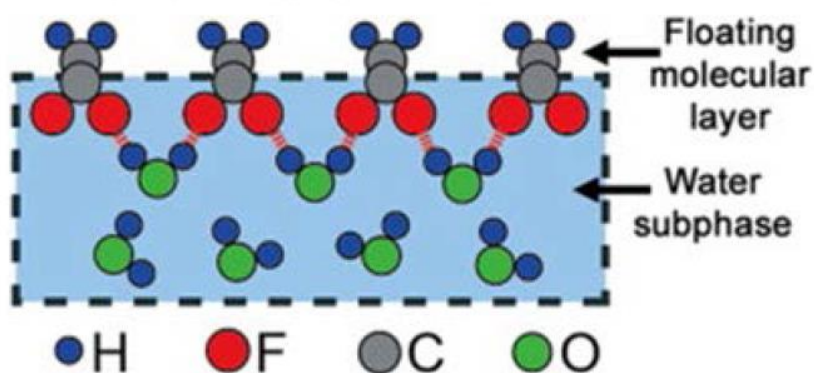


**Figure 3.2:** PVDF monolayer spread on the water subphase [2].

---

Langmuir monolayer formation is achieved by constant rate compression of the barriers. The compression isotherm experiments are performed at 18 °C to know the effect of spreading solution and barrier speed (10, 20, 32 mm/min) on the as formed Langmuir monolayers.

The information about the configuration retention of the monolayer for different barrier speeds is determined by 5 cycle pressure-area isotherm hysteresis experiments.

**5. Oscillating Barrier experiments:** The visco-elastic properties of the Langmuir monolayers are studied with oscillating barrier experiments.

The barriers are oscillated at 10 different frequencies ranging from 5 mHz to 55 mHz to find out the most suitable frequency for oscillation experiments at temperature 18 °C with barrier speed for compression isotherm of 20 mm/min.

The barrier oscillation experiment for Langmuir monolayers is performed for different molarities with most suitable frequency of 30 mHz for barrier oscillation at temperature 18 °C with barrier speed of 20 mm/min. by spreading solution of 50 µl on the water surface.

The barrier oscillation experiments for different barrier speeds is carried out at temperature of 18 °C with 0.0936 mol/l PVDF spreading solution keeping the oscillating barrier frequency at 30 mHz.

**6. Substrate preparation:** The borosil glass slides are used as a substrate and are thoroughly cleaned with piranha cleaning which involves the cleaning of glass slide in the boiling solution of sulphuric acid and hydrogen peroxide (in 7:3 ratio respectively). Then the glass slides are ultrasonicated in acetone, methanol, type-3 ultra-pure water for five minutes respectively.

**7. Langmuir-Blodgett thin film deposition:** The glass substrate is dipped in the subphase attached with dipper control clip for the deposition of the monolayer formed on the subphase. The dipping is performed at upstroke speed of 2 mm/min with wait time of 1 min and downstroke speed of 15 mm/min without any wait time, depositing one layer at a time. The subphase is changed everytime for the deposition of the next new layer.

**8. Drying and annealing of the thin film sample:** The PVDF thin film deposited on the glass substrate is dried in vacuum and annealed at 145°C for 4 hours for final phase formation [3].

---

9. Final PVDF thin film samples prepared after annealing are given in table 3.1 as follows:

**Table 3.1:** PVDF samples prepared.

Barrier Speed(mm/min)	No. of Layers deposited
20	1
20	3
20	8

The thin films prepared are characterized by the characterization techniques discussed below in the section 3.4.

### 3.3 Langmuir-Blodgett Method

The method involved for the preparation of PVDF thin films is the Langmuir-Blodgett method. It is the method for deposition of the thin monolayers on a solid substrate. It allows us to deposit a number of monolayers or multilayers on a solid substrate layer by layer. The layer of the material formed upon the subphase is what is known as a Langmuir monolayer and this monolayer when deposited on a solid substrate is known as Langmuir-Blodgett films [4].

For the material to be well suited for the deposition with Langmuir-Blodgett technique, it should be amphiphilic in nature (figure 3.3) [5].

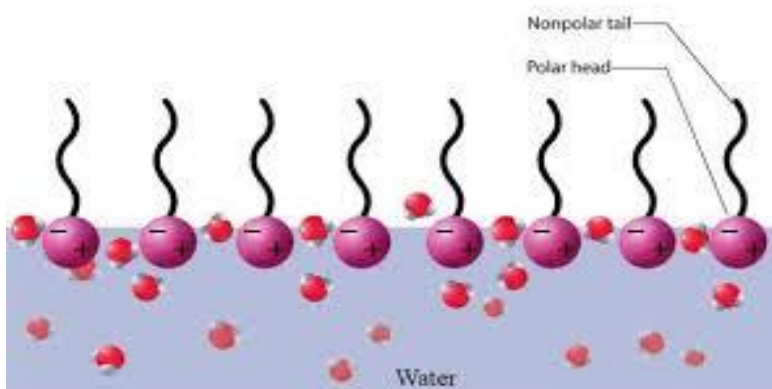


**Figure 3.3:** Amphiphilic molecule accordant for Langmuir-Blodgett method [6].

#### 3.3.1 Assembly of Langmuir-Blodgett technique

The Langmuir-Blodgett technique consists of following components which help in the formation of the thin films on the subphase figure 3.4.

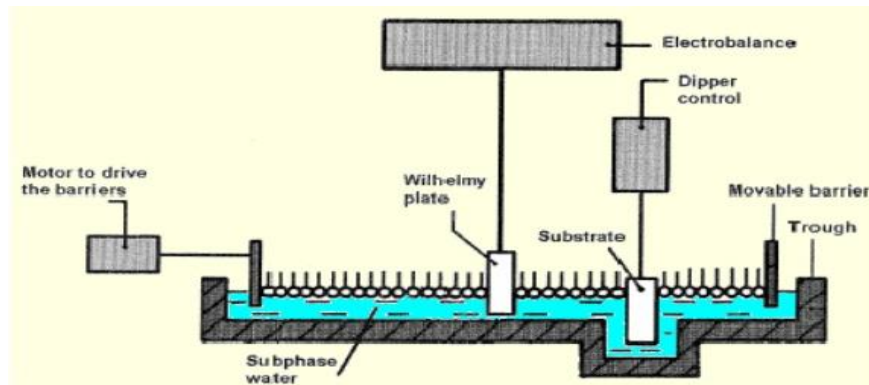


**Figure 3.4:** Assembly of Langmuir-Blodgett method [4]

1. **Trough:** The trough is made up of Teflon polymer. The surface of the trough has a vertical depression in it which is known as the dipping well for the deposition of thin film. The trough surface is supported with aluminium base which contains the water flow channels for the regulation of the water at a particular temperature on the trough surface.
2. **Barriers:** The barriers are used for the compression of the monolayer spread at the air-water interface on the trough. The barriers are movable in nature and hence when moves inward the film undergoes compression and when the barriers move outward the film undergoes expansion.
3. **Electrobalance:** The electrobalance consists of Wilhelmy plate which monitors the surface pressure of the monolayer on the subphase. It is the thin hydrophilic plate which senses the pressure changes that occur on the thin layer spread on the subphase.
4. **Dipper control:** The dipper control controls the dipping action of the monolayer on the substrate. The substrate used for the dipping can be either hydrophilic or hydrophobic in nature depending upon the type of substrate [7].

### 3.3.2 Fabrication and deposition of Langmuir monolayer

The thin films are formed when the amphiphilic molecules are spread on the air-water interface on the subphase. The molecules align themselves in such a manner that the hydrophilic part is attracted towards the subphase and the long hydrophobic tail is vertically away from the subphase as the area per molecule of the film decreases. For the fabrication of the Langmuir monolayer, the Langmuir accordant material is dissolved in a suitable solvent and then spread on the water subphase. Once the solvent evaporates, the movable barriers are moved inwards and the film undergoes compression. The molecules are arranged in a random manner on the subphase and the area per molecule available is maximum initially. As the barrier are moved the

---

gas phase is achieved first, followed by liquid and solid phase depending upon the mean molecular area available per molecule [4].

When Langmuir monolayers are deposited on a solid substrate, a thin film is formed on the substrate and is known as Langmuir-Blodgett film. The substrate can be hydrophilic or hydrophobic. The substrate is clipped with the dipper control and can be dipped vertically to coat it with the thin film. There should be fixed surface pressure throughout the dipping [4].

### 3.3.3 Types of Deposition

The multilayer Langmuir-Blodgett thin films can be deposited on the solid substrate with three types. These are:

- a) **X-type deposition:** In the X-type deposition, the hydrophobic tails of the thin film is attached to the substrate in the downstroke as first layer and further the tails are attached to the subsequent hydrophilic heads and forms the second layer.
- b) **Y-type deposition:** In the Y-type deposition, the first layer is formed when the hydrophilic heads of the thin film is attached to the substrate in the upstroke and then with the downstroke, the hydrophobic tails are attached to the subsequent hydrophobic tails and forms the second layer.
- c) **Z-type deposition:** In the Z-type deposition, the hydrophilic heads are attached to the substrate with the upstroke and form the first layer and further the hydrophilic heads are attached with the subsequent hydrophobic tails and form the second layer [8].

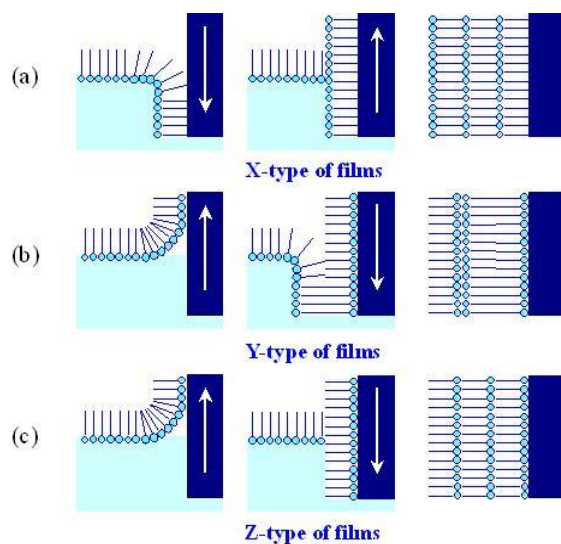


**Figure 3.5:** Types of deposition [5]

### 3.3.4 Transfer Ratio

Transfer ratio is defined as the ratio which depicts how much of the thin film has been deposited on the solid substrate during the dipping process. It is the ratio of the amount of film that is deposited on the substrate to the total amount of film present on the subphase. For a film with good adhesion, the transfer ratio is usually lies between (0.90 to 1.00) [8].

## 3.4 Characterization Techniques

The thin films deposited on the solid substrate are characterized in order to study various properties of the material. The various characterization techniques involved in the study of thin films are as follows:

### 3.4.1 Surface pressure-area ( $\Pi$ -A) isotherm

An inward pull is experienced by the molecules on the surface due to uneven bonding interactions of the surface molecules which produces a tension on the surface of the thin film. This is termed as surface tension and is denoted by ‘ $\gamma$ ’. When the molecules of the monolayer undergo compression, the surface pressure of the monolayer is affected due to the interactions of the molecules with each other. This is given by the expression,

$$\Pi = \gamma_0 - \gamma \quad \dots\dots\dots(3.1)$$

Where  $\Pi$  is surface pressure,  $\gamma$  is the surface tension of the subphase without monolayer and  $\gamma_0$  is the surface tension of the subphase with monolayer. The area per molecule depicts the area available for each molecule on the subphase. The surface pressure-area isotherm is always performed at a constant temperature and is depicted in the figure 3.6 below:

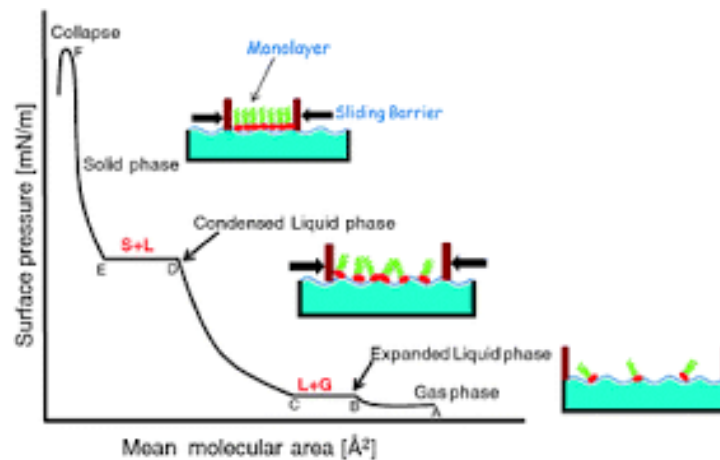


**Figure 3.6:** Surface pressure-area isotherm [9]

The film undergoes a change in the surface pressure with compression. Firstly, the molecules are randomly arranged and hence are away from each other. This is the gas phase. With further compression, the molecules arrive close to each other and hence interaction between them takes place. This forms the liquid phase. The compressibility changes remarkably when the molecules are further compressed and reach the solid phase and there is sharp rise in the slope of curve and the compressibility is given by

$$C = -\frac{1}{A} \frac{\partial A}{\partial \pi} \dots\dots\dots(3.2)$$

Where A is the area of the solid phase and  $\Pi$  is the surface pressure. The area per molecule in the solid phase is least and hence with further compression the film breaks and the molecules of the monolayer accumulate over each other.

The static elasticity is defined as the reciprocal of compressibility and is given by

$$E = -A \frac{d\pi}{dA} \text{ (mN/m)} \dots\dots\dots(3.3)$$

The surface pressure-area isotherms are very important as they depict various properties of the thin film which are helpful to study the material [8].

### 3.4.2 Hysteresis

The form retention of the surface pressure-area isotherms is determined by the hysteresis of the monolayer. In hysteresis, the isotherm is compressed and expanded consecutively for a particular number of cycles. Figure 3.7 shows the hysteresis curve.

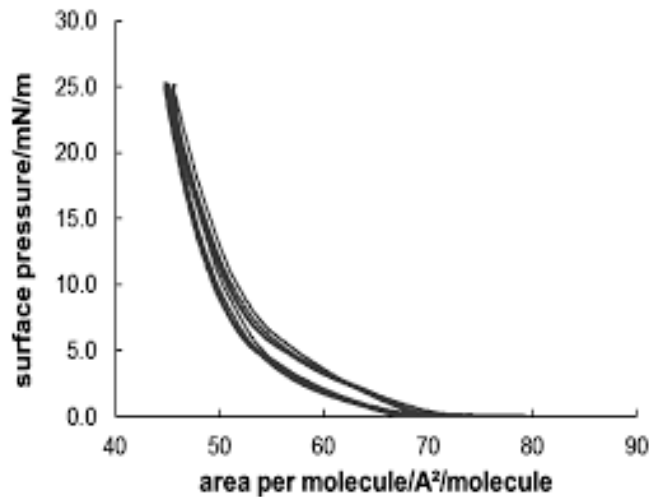


**Figure 3.7:** Hysteresis curves for Langmuir monolayer [10]

---

If the isotherm repeats itself after each consecutive cycle then the material is quite stable and has a good stability. The hysteresis curve also reveals how stable is the thin film formed on the subphase as it undergoes compression and expansion simultaneously [11].

### 3.4.3 Barrier Oscillation

Barrier oscillation is the phenomenon to study the visco-elastic properties of the thin film. The barrier oscillation is performed at a particular surface pressure which kept constant throughout the oscillations after the surface pressure of the isotherm is reached. The barriers are oscillated at a particular frequency once the target surface pressure is reached. It helps us to determine the dynamic elasticity of the thin film and is given by

$$G = G\cos\theta + G\sin\theta \quad \dots\dots\dots(3.4)$$

$$G = G' + G'' \quad \dots\dots\dots(3.5)$$

Where  $G\cos\theta = G'$  is the real part and gives storage elastic modulus and  $G\sin\theta = G''$  is the imaginary part and gives the loss modulus.

The loss angle is given by  $\text{loss angle} = \frac{G''}{G'}$  .....(3.6)

Higher the  $G''$ , higher the film is condensed [11].

### 3.4.4 Atomic Force Microscopy (AFM)

Atomic Force Microscopy (AFM) is defined as the process in which a tip attached to the cantilever scans the surface area of the thin film in the raster fashion and helps to give the topographical information about the thin film. The force between the tip and the sample is measured and then is transformed to the three-dimensional image which is projected on the screen. The atomic force microscopy induces a force on the sample as the tip is touched with it and hence is called as force microscopy. The AFM can be operated in two modes i.e. tapping mode and non-tapping mode [12]. Figure 3.8 (a) shows the schematic of Atomic Force Microscopy (AFM) and figure 3.8 (b) shows the laboratory view of AFM.

The AFM is performed for various PVDF thin films samples prepared with varied number of layers (1, 3, 8 layers) in non-contact mode on NT-MDT Solver Next. The topographical view of the surface of PVDF thin film is obtained and roughness value is measured.

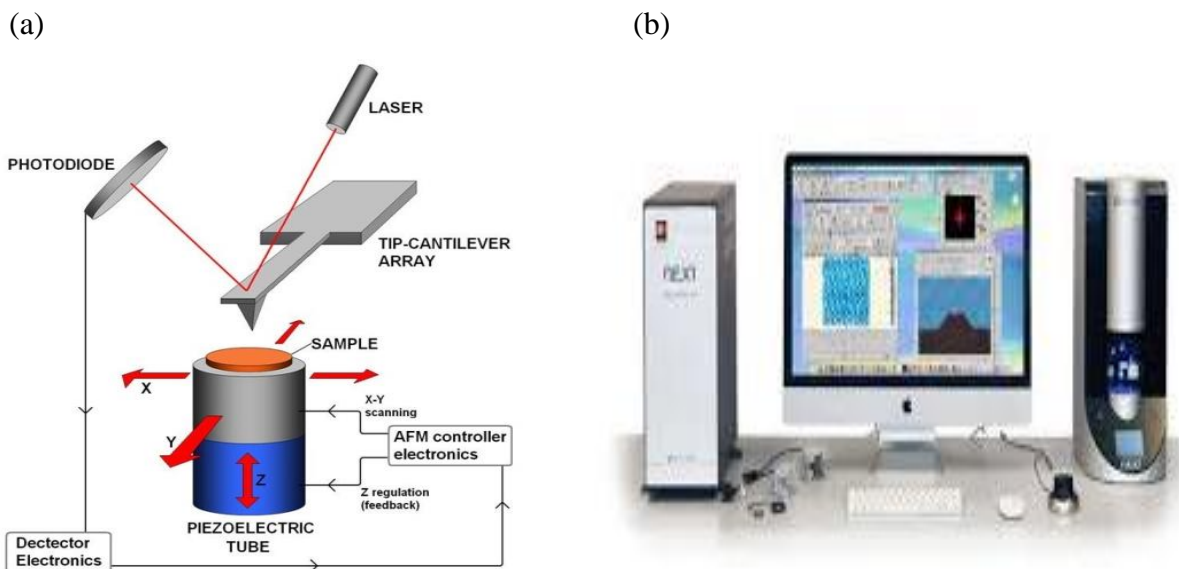


**Figure 3.8:** (a) Schematics of Atomic Force Microscopy [12], (b) Laboratory view of AFM [13]

### 3.5 References

1. Chandan Kumar et al., *European Polymer Journal*, 86 (2017) 132-142.
2. Subrata Maji et al., *Phys. Chem. Chem. Phys.*, 17 (2015) 8159-8165.
3. Liuxia Ruan et al., *Polymers*, 10(3) (2018) 228.
4. Osvaldo N. and Oliveira Jr., *Brazilian Journal of Physics*, 22(2), (1992), 60-68.
5. Syed Arshad Hussain, Deptt. of Physics, Tripura University.
6. K. Panjabi, R. Rudra, 6 (2016), 13.
7. Manual KSV NIMA Langmuir and Langmuir-Blodgett deposition troughs.
8. G. Roberts, *Langmuir Blodgett Films*, Plenum press, New York, 1<sup>st</sup> edition (1990).
9. Zimple Matharu et al., *Chem. Soc. Rev.*, 41 (2012) 1363-1402.
10. Benjamin Weber, *Polymers*, 8 (2016) 427.
11. Choudhary Raveena, Brar Loveleen Kaur (Guide), Effect of pH on the Langmuir monolayer of zirconyl stearate and the synthesized zirconium oxide thin films, Master theses@ SPMS, TuDR, (2017).
12. Cheryl R. Branchard, *Journals springer*, 1 (1996).
13. Atomic force microscope- NT-MDT solver next instrument.

## Overview

In this chapter, the experimental results obtained from the characterization techniques such as surface pressure-area isotherms, hysteresis experiments, oscillating barrier experiments, atomic force microscopy (AFM) are analyzed and discussed.

### 4.1 Surface Pressure – Area ( $\Pi$ -A) Isotherms

The  $\Pi$ -A isotherms are basic in understanding the Langmuir monolayer properties of the material.

#### 4.1.1 Effect of Molarity of the spreading solution

The effect of molarity change of the spreading solution is analyzed for six different molarities. Figure 4.1 (a) shows the variation in  $\Pi$ -A isotherms with the spreading solution molarity. Table 4.1 gives the values of the mean molecular area (MMA) for the liquid and solid phases as well as the static elastic constant for the solid phase obtained for each isotherm.

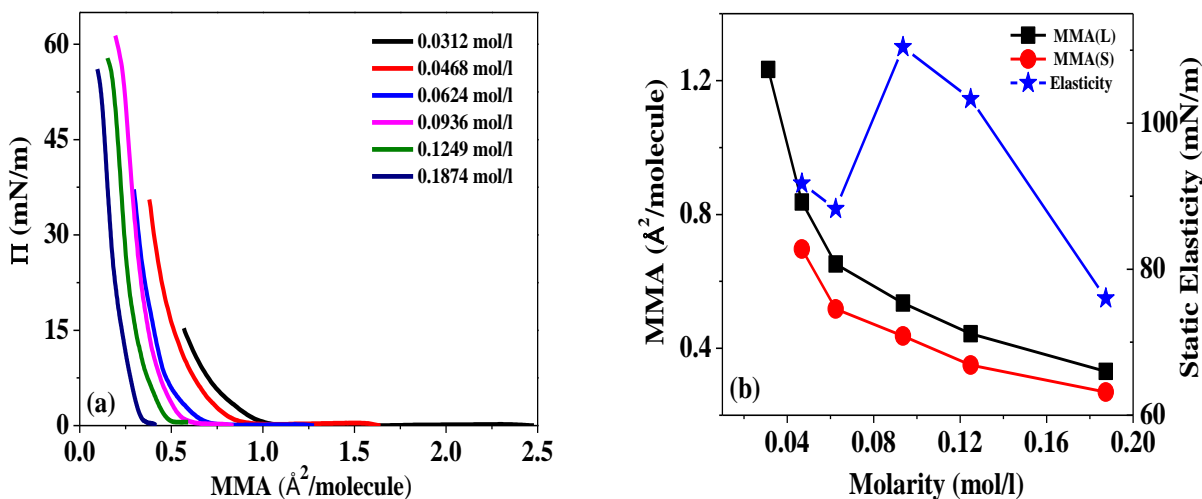


**Figure 4.1:** (a)  $\Pi$ -A isotherms for different molarities of PVDF dissolved in NMP on DI water as subphase at temperature 18°C, spreading solution volume of 50  $\mu\text{l}$  and barrier speed of 30 mm/min., and (b) variation of mean molecular area of liquid and solid phase (MMA) and elasticity with different molarities.

**Table 4.1:** Values of mean molecular area for liquid phase ( $MMA_L$ ) and solid phase ( $MMA_S$ ) with static elasticity of solid phase for different molarities of PVDF in the spreading solution.

Molarity of PVDF (mol/l)	$MMA_L$ ( $\text{\AA}^2/\text{molecule}$ )	$MMA_S$ ( $\text{\AA}^2/\text{molecule}$ )	Static Elasticity (mN/m)
0.0312	1.233	-	-
0.0468	0.837	0.696	91.7
0.0624	0.652	0.517	88.2
0.0936	0.535	0.437	110.4
0.1249	0.444	0.350	103.3
0.1874	0.331	0.269	76.0

The effect of spreading solution molarity on the isotherms is clearly visible in figure 4.1 (a). This indicates the presence of high degree of interactions between PVDF monomers which are being modified by the concentration PVDF in the initial solution. It is observed that as the molarity of the spreading solution increases the MMAs for the liquid as well as the solid phase decreases steadily (figure 4.1 (b)). This is easily explained by availability of more number of molecules. A more interesting result emerges from the analysis of the static elastic constant of the solid phase. Initially for 0.0312 mol/l PVDF spreading solution the complete solid phase is not achieved even for complete closure of the barriers. As the conc of PVDF is increased in the spreading solution the solid phase formation starts and the static elastic constant shows a peak for 0.0936 mol/l spreading solution. So the initial increase in PVDF concentration helps to enhance the interactions between the monomers and formation of strong solid films. A further increase in the concentration of the spreading solution results in films having lower MMA as well as elastic constant. This indicates that for very large concentration of the PVDF the solid films have net reduced stability which may have resulted from repulsions between different monomers due to proximity of the dipoles.

High value of static elastic constant (110.41 mN/m) for 0.0936 mol/l spreading solution indicates that the films formed for this concentration are more stable and should perform better during dipping/transfer experiments [5]. So we choose this concentration for all further experiments.

#### 4.1.2 Effect of Barrier Speed

The effect of barrier speed on the PVDF monolayer formation was analyzed for different barrier speeds during compression. The  $\Pi$ -A isotherms and elasticity curves for different barrier speeds

are shown in figure 4.2 (a). Table 4.2 shows the values of mean molecular area for liquid phase and solid phase with different barrier speed.

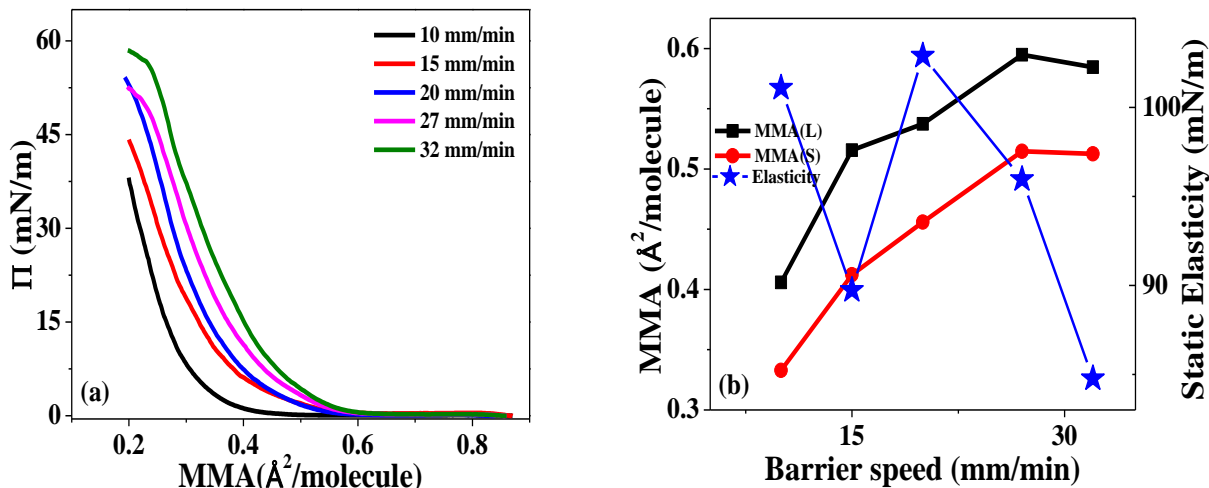


**Figure 4.2:** (a)  $\Pi$ -A isotherms for different barrier speed of 0.0936 mol/l PVDF spreading solution at temperature 18°C and spreading solution volume of 50  $\mu$ l and (b) variation of mean molecular area of liquid and solid phase (MMA) and elasticity with different barrier speeds.

**Table 4.2:** Values of mean molecular area of liquid phase ( $MMA_L$ ) and solid phase ( $MMA_S$ ) and static elasticity of solid phase for different barrier speeds during compression.

Barrier speed (mm/min)	$MMA_L$ ( $\text{\AA}^2/\text{molecule}$ )	$MMA_S$ ( $\text{\AA}^2/\text{molecule}$ )	Static Elasticity (mN/m)
10	0.406	0.332	101.0
15	0.516	0.412	89.7
20	0.537	0.456	102.8
27	0.595	0.515	95.9
32	0.585	0.513	84.7

From the above analysis, it is observed that as the barrier speed is increased, the mean molecular area (MMA) for liquid and solid phase increases (figure 4.2(b)). For barrier speed of 10 mm/min, the value of MMA for liquid and solid phase is lowest and it increases gradually with the increase in the barrier speed during compression. This can be explained by invoking the kinetics of the monomers on the subphase surface. If the barrier speed is slow the monomers have more time available to achieve the best configuration in the monolayer with most compaction. The value of MMA for liquid and solid phase remains almost constant for barrier speed 27 mm/min and 32 mm/min. This implies that for these and higher speeds the monomers are not allowed any

---

time to achieve favorable configurations in the monolayer. This is also supported by the decrease in the elasticity as the barrier speed increases. The peak in the static elasticity with the value of 102.8 mN/m is observed at a barrier speed of 20 mm/min which indicates a monolayer of highest stability. This clearly indicates that the slow compression speed may have resulted in stearically compact films but the repulsion between the partially charged fluorine atoms on the neighbouring monomers is actually reducing the strength of the films. The 10 mm/min films seem comparable so more experiments were performed – hysteresis and oscillating barriers to determine which films were better.

From the above data it is determined that films formed with the barrier speed of 20 mm/min are more stable and should perform better during dipping/transfer experiments. So we choose this barrier speed for all further experiments.

## 4.2 Hysteresis analysis of $\Pi$ -A isotherms

The form retention of the monolayers formed from different compression speed is tested by the hysteresis analysis of the  $\Pi$ -A isotherms. The 5 cycles of the hysteresis curve data for barrier speeds 30 mm/min is shown in the figure 4.3. This data is representative of all the hysteresis curves obtained. Table 4.3 and 4.4 shows the MMAs and static elasticity values obtained from the analysis of the data for all the barrier speeds (10, 20, 30 mm/min).

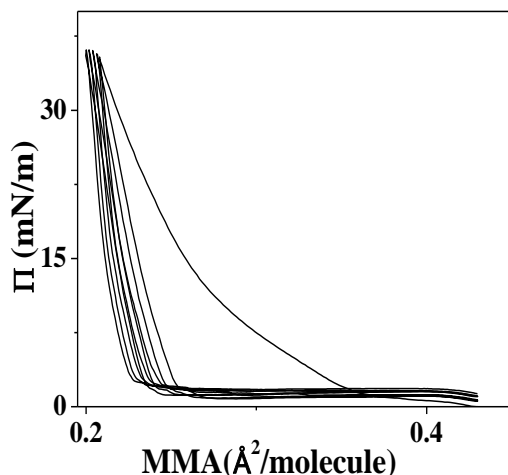


**Figure 4.3:** Hysteresis curves showing variation of surface pressure with MMA for barrier speed 30 mm/min at temperature 18°C.

**Table 4.3:** For barrier speeds (10, 20 and 30) mm/min values of mean molecular area of liquid phase ( $MMA_L$ ) and solid phase ( $MMA_S$ ).

Cycle no.	$MMA_L$ ( $\text{\AA}^2/\text{molecule}$ )	$MMA_S$ ( $\text{\AA}^2/\text{molecule}$ )	$MMA_L$ ( $\text{\AA}^2/\text{molecule}$ )	$MMA_S$ ( $\text{\AA}^2/\text{molecule}$ )	$MMA_L$ ( $\text{\AA}^2/\text{molecule}$ )	$MMA_S$ ( $\text{\AA}^2/\text{molecule}$ )
	10 mm/min		20 mm/min		30 mm/min	
1	0.264	0.173	0.286	0.227	0.411	0.310
2	0.223	0.174	0.274	0.244	0.264	0.250
3	0.180	0.162	0.275	0.252	0.259	0.243
4	0.179	0.155	0.261	0.240	0.249	0.238
5	0.176	0.146	0.254	0.222	0.252	0.235

**Table 4.4:** Values of static elasticity of solid phase for consecutive cycles of compression.

Cycle no.	Static Elasticity (mN/m)	Static Elasticity (mN/m)	Static Elasticity (mN/m)
	10 mm/min	20 mm/min	30 mm/min
1	102.4	109.8	109.6
2	216.8	96.5	204.0
3	512.6	100.8	222.0
4	113.8	106.8	239.2
5	123.9	155.5	254.0

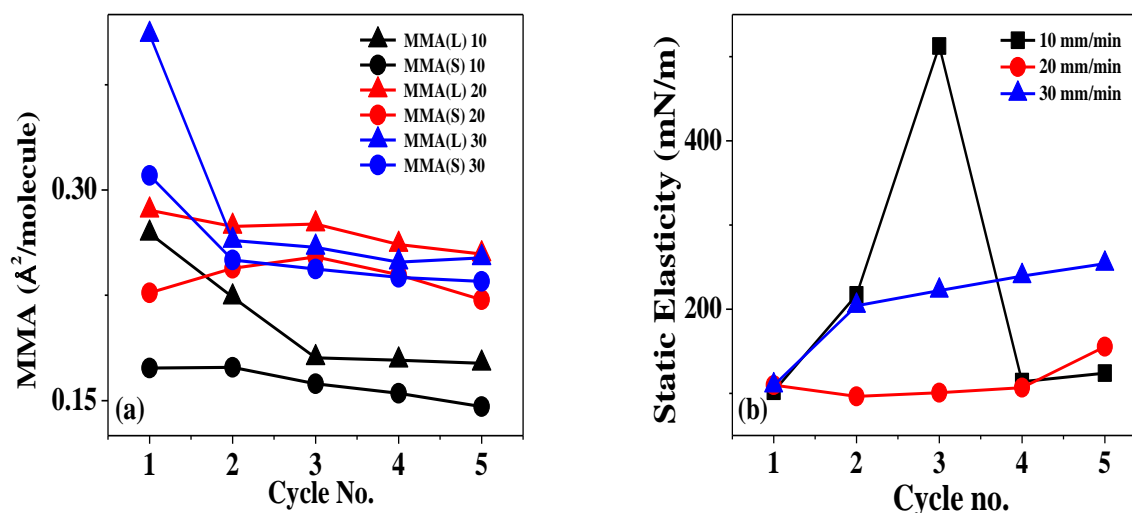


**Figure 4.4:** (a) Variation of liquid phase and solid phase with cycle no. for barrier speed (10, 20 and 30) mm/min, (b) variation of static elasticity with cycle number for different barrier speeds.

The hysteresis analysis of the PVDF monolayers for different barrier speeds showed difference in the shape retaining of the monolayer formed for the different compression and expansion

---

speeds. More the reproducibility of the isotherm for each cycle more is the stability of the isotherm. A sudden decrease in the value of MMA is observed after the initial cycles of compression for barrier speed of 10 mm/min and 30 mm/min. and thereafter the value of MMA remains almost constant. For the barrier speed 20 mm/min the Mean molecular area (MMA) for liquid and solid phase remains almost constant for various cycles of compression. Moreover, from the above analysis it is evident that the static elasticity does not change much with compression cycles and hence remains almost constant for 20 mm/min barrier speed.

Hence, it seems that the most suitable barrier speed at which maximum formation retention of the isotherms takes place is 20 mm/min and is considered further for dipping experiments.

### **4.3 Barrier oscillation**

The barrier oscillation was performed firstly for various frequencies to select the most suitable frequency for barrier oscillation experiments of PVDF monolayers.

#### **4.3.1 Effect of various frequencies on barrier oscillation**

The PVDF spreading solution used is of 0.0936 mol/l molarity. The set of frequencies taken was ranging from 5 mHz to 55 mHz with an interval of 5 mHz. Figure 4.5 shows the stacked graph for surface pressure variation with time for various frequencies. Table 4.5 shows the values of dynamic viscoelastic properties of the curves obtained with barrier oscillation experiment.

The analysis shows that, the value of  $|G|$ ,  $G'$ ,  $G''$  first decreases and then increases after frequency 10 mHz and then suddenly drops at frequency 25 mHz. At frequency 30 mHz the value of  $G''$  is minimum but the corresponding value of  $G'$  is maximum and hence gives the best stability. The value of  $G''$  then increases and decreases in alternate fashion for the next values of frequencies. This shows that the suitable value for the analysis of barrier oscillation of PVDF monolayers is 30 mHz and is kept fixed for analysis of monolayers for spreading solution molarity and barrier speed change.

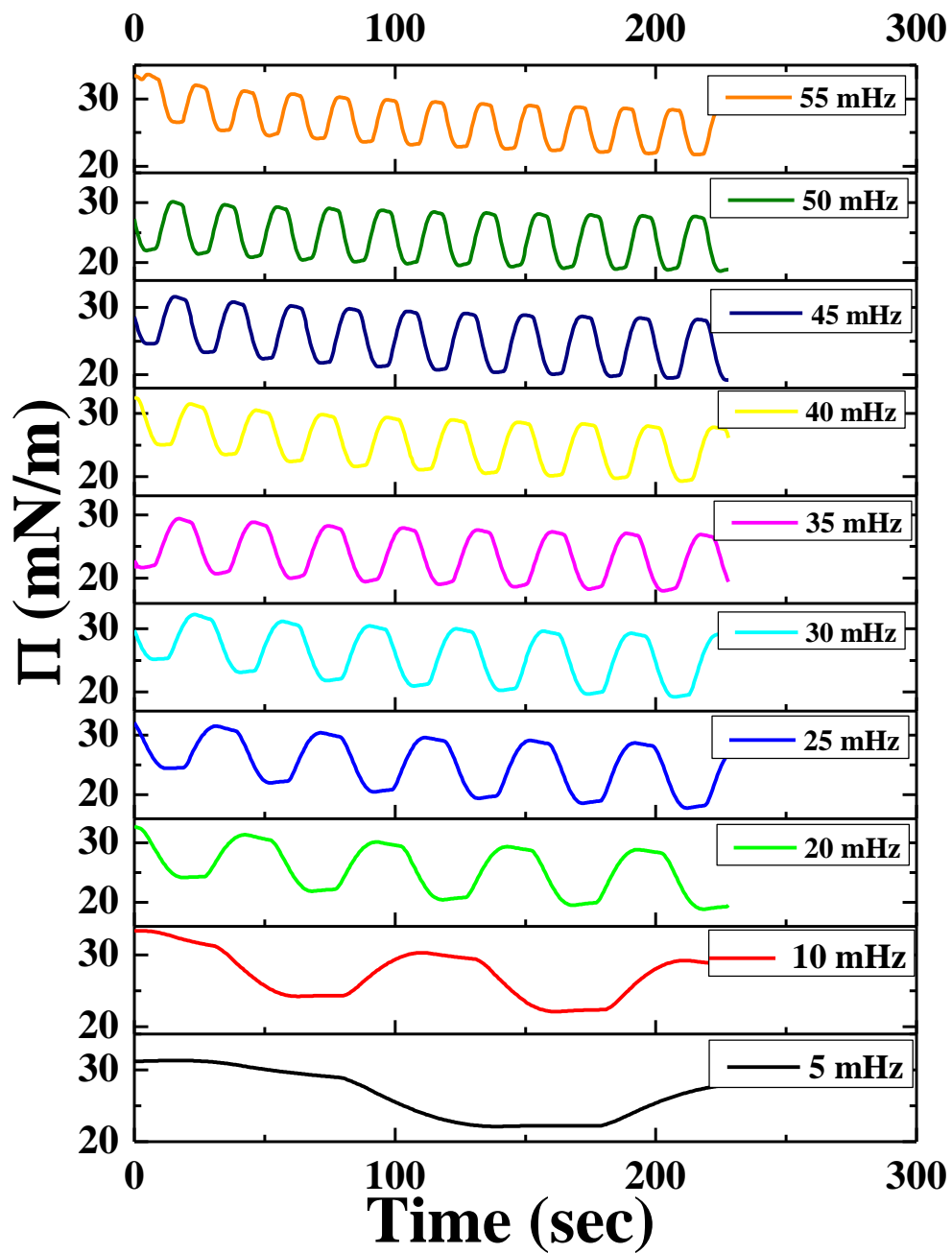


**Figure 4.5:** Surface pressure variation with time for different frequencies at temperature 18°C and 20 mm/min barrier speed.

**Table 4.5:** Values of  $|G|$ ,  $G'$ ,  $G''$  for various frequencies of barrier oscillation.

Frequency (mHz)	$ G $ (mN/m)	$G'$ (mN/m)	$G''$ (mN/m)
5	255.68	237.06	95.77
10	194.81	189.61	44.70
20	220.18	198.39	95.53
25	161.56	161.51	4.15
30	189.03	188.59	12.88
35	188.12	110.41	152.32
40	188.72	172.01	77.63
45	118.97	179.71	378.47
50	134.77	120.55	60.27
55	86.55	73.06	46.40

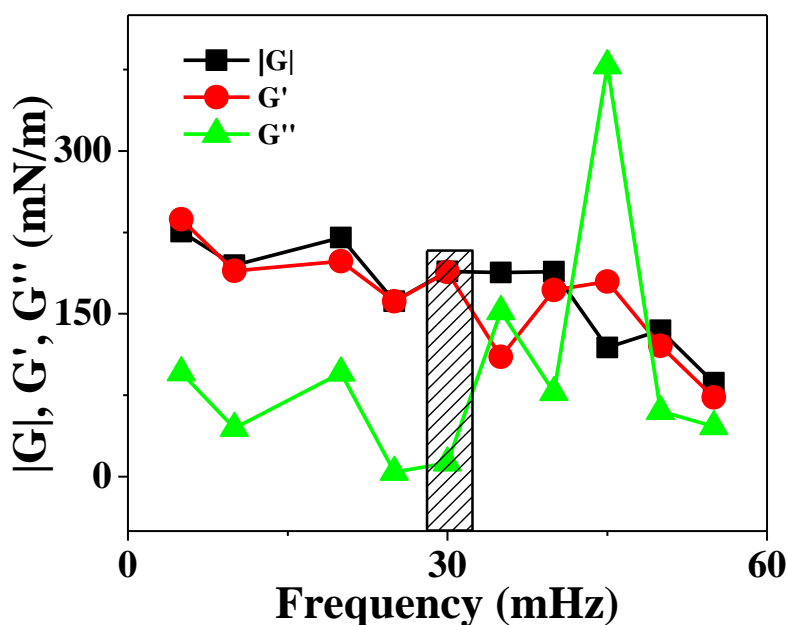


**Figure 4.6:** Graph showing the variation for  $|G|$ ,  $G'$ ,  $G''$  with various frequencies.

### 4.3.2 Effect of different molarities of PVDF with barrier oscillation

The effect of different molarities of PVDF with barrier oscillation is studied at 20 mm/min. Figure 4.7 shows the stacked graph for the variation of surface pressure with time for different molarities. Table 4.6 shows the values of visco elastic properties is given below:

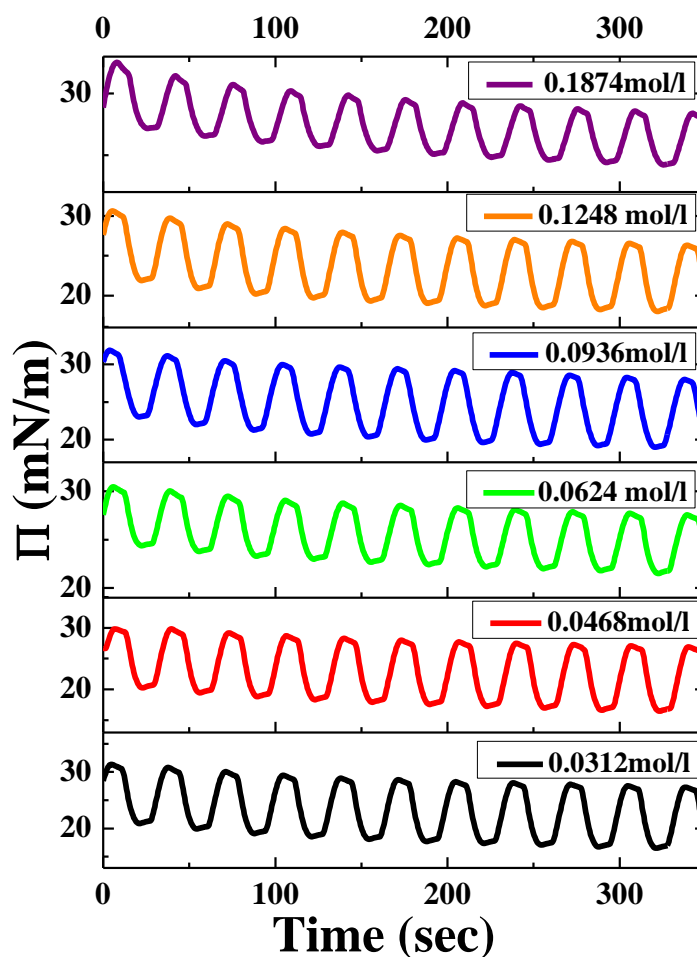


**Figure 4.7:** Variation of surface pressure with time for different molarities at temperature 18°C and 20 mm/min barrier speed with frequency for barrier oscillation at 30 mHz.

**Table 4.6:** Values of  $|G|$ ,  $G'$ ,  $G''$  for different molarities of PVDF of barrier oscillation.

Molarity (mol/l)	$ G $ (mN/m)	$G'$ (mN/m)	$G''$ (mN/m)
0.0312	480.66	202.26	436.04
0.0468	209.73	8.95	209.54
0.0624	319.28	134.63	289.51
0.0936	189.24	171.97	78.97
0.1249	122.62	43.42	114.68
0.1874	553.30	169.84	526.59

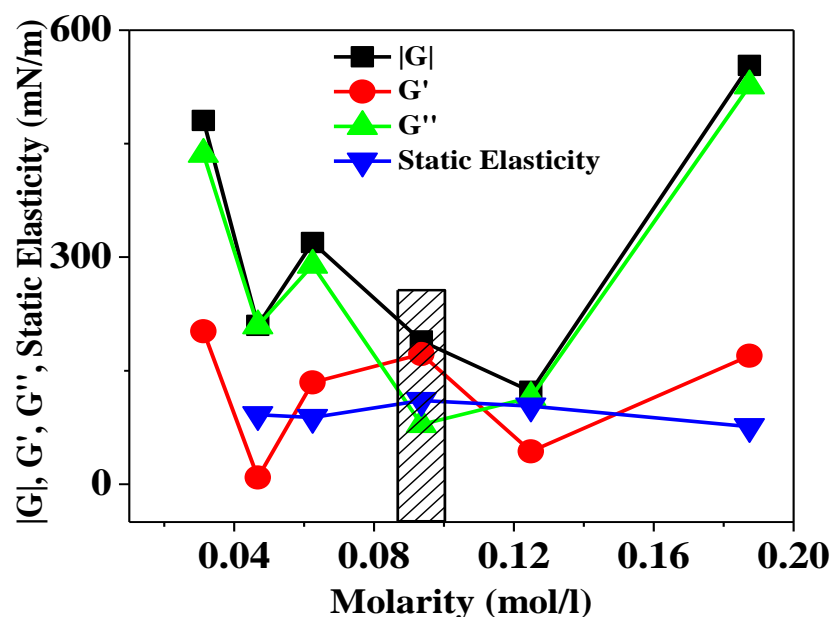


**Figure 4.8:** Graph showing the variation of static elasticity,  $|G|$ ,  $G'$ ,  $G''$  with variation in molarity.

Form the above analysis, it is clear that as the value of  $G'$  and  $G''$  vary in the same manner for different molarities of PVDF sample. But at a particular molarity, 0.0936 mol/l, it is evident that the value of  $G'$  is maximum while the corresponding value of  $G''$  is minimum. At this molarity the value of static elasticity is maximum and hence, it is the most suitable molarity for the dipping/transfer experiments.

### 4.3.3 Effect of barrier speed change with barrier oscillation

The effect of barrier speed change with barrier oscillation is studied by varying the barrier speed at a given frequency. Figure 4.8 shows the stacked graph for the variation of surface pressure with time for different barrier speeds at a given frequency. Table 4.7 shows the values of visco elastic properties as given below:

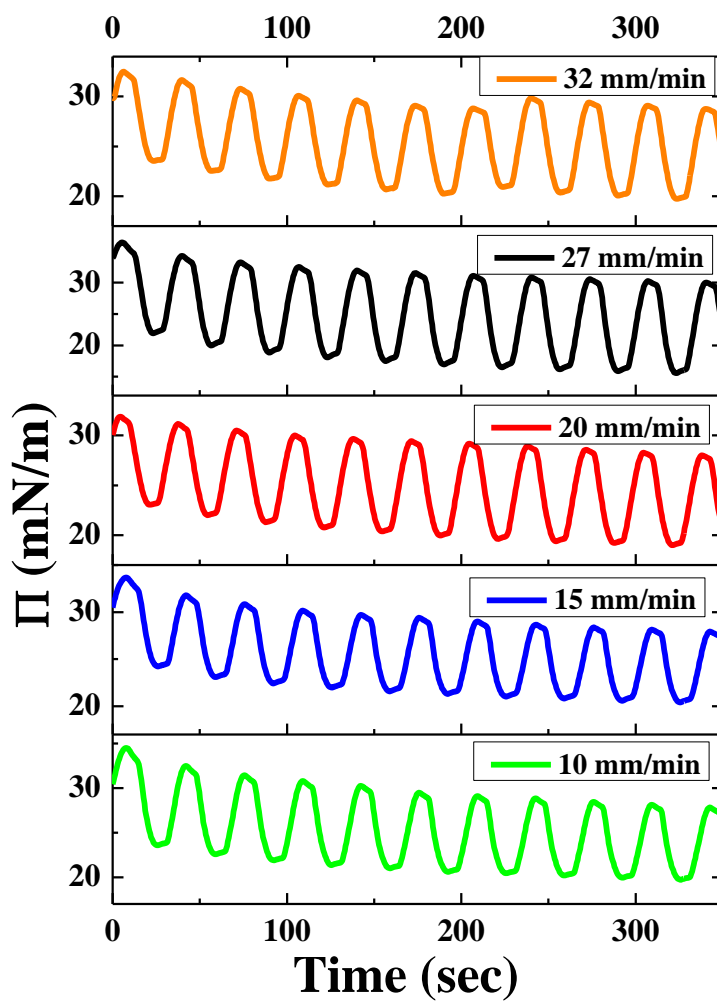


**Figure 4.9:** Variation of surface pressure with time for barrier speed change at temperature 18°C and barrier speed of 20 mm/min with frequency for barrier oscillation at 30 mHz.

**Table 4.7:** Values of  $|G|$ ,  $G'$ ,  $G''$  for different barrier speeds of compression.

Barrier speed (mm/min)	$ G $ (mN/m)	$G'$ (mN/m)	$G''$ (mN/m)
10	123.34	122.41	15.15
15	177.35	139.22	109.87
20	189.24	171.97	78.97
27	474.30	361.40	307.16
32	137.27	133.50	31.96

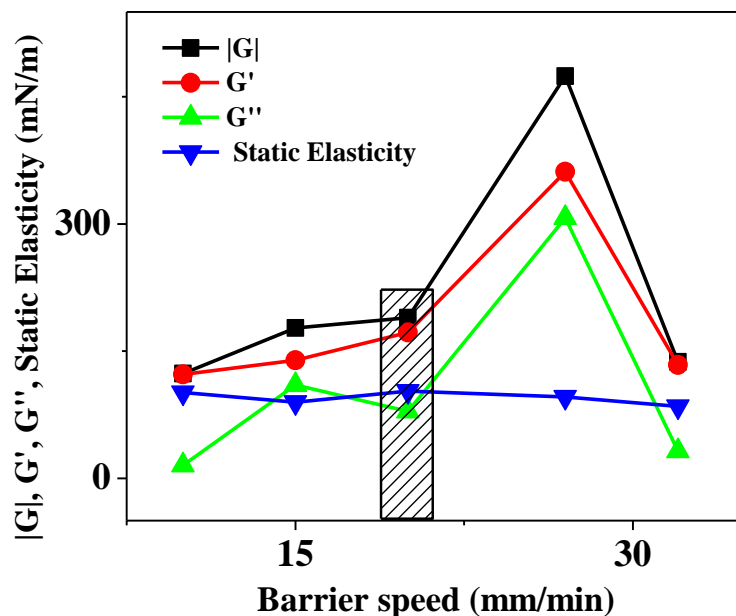


**Figure 4.10:** Graph showing variation of static elasticity,  $|G|$ ,  $G'$ ,  $G''$  with different barrier speeds.

The above analysis indicates that the value  $G'$  and  $G''$  increases and decreases in the alternate fashion with various barrier speeds. The value of  $G''$  was maximum at barrier speed 27 mm/min. But at a particular barrier speed of 20 mm/min., it is evident that the value of  $G'$  is maximum while the corresponding value of  $G''$  is minimum. At this barrier speed the value of static elasticity is maximum and hence, it seems that the most suitable barrier speed for the dipping/transfer experiments is 20 mm/min.

**Final dipping parameters:** PVDF langmuir monolayers on the water subphase at 18 °C were characterized completely using static  $\Pi$ -A isotherms, hysteresis as well as the dynamic oscillating barrier techniques to determine the trough parameters for the most stable PVDF monolayer:

Spreading solution concentration: 0.0936 mol/l

Compression rate: 20 mm/min

Also all the depositions were started with the hydrophilic glass substrate already dipped in the subphase before the spreading of the PVDF monolayer. So, first movement of the dipper is always upstroke.

---

#### 4.4 Deposition of PVDF Langmuir-Blodgett thin films

The PVDF Langmuir-Blodgett thin films are deposited on the hydrophilic glass substrate. The glass substrate is first deposited with PVDF with 10 deposition cycles giving 10 transfer ratio (TR). Various experiments for dipping are performed to set the parameters for dipping. These are as follows:

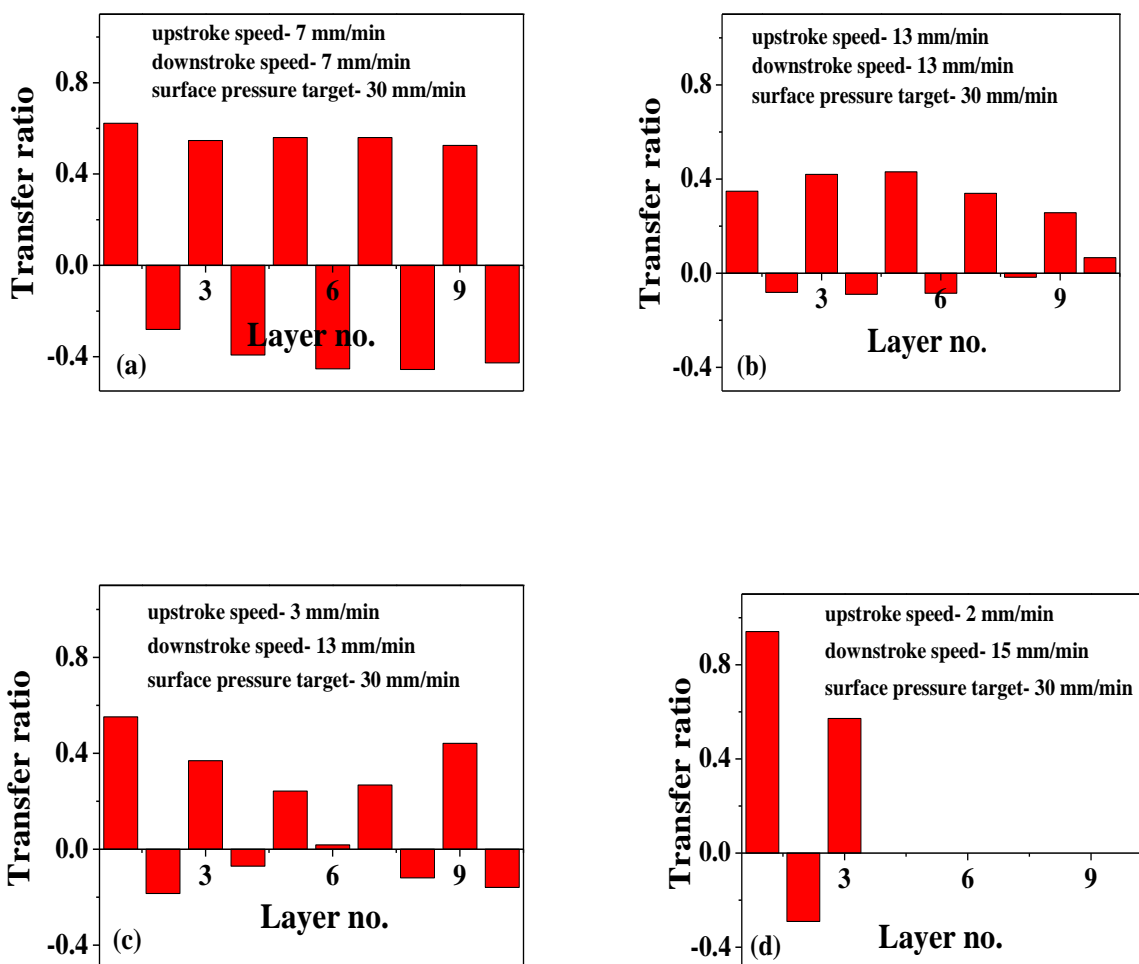


**Figure 4.11:** (a), (b), (c), and (d) graphs shows the variation of Transfer ratio with layer number at temperature 18 °C with barrier speed of 20 mm/min. and spreading 100  $\mu$ l of 0.0936 mol/l PVDF spreading solution.

From the above conditions, it is observed that the TR of 0.5 is achieved with upstroke and downstroke speed of 7 mm/min. and it decreased with the upstroke and downstroke speed of 13

---

mm/min. With upstroke speed of 3 mm/min. and downstroke speed of 13 mm/min. the TR of 0.6 achieved. For dipping speed up 2 mm/min and down 15 mm/min, maximum transfer ratio (0.94) is observed for upstroke (first layer) with barrier speed of 20 mm/min. A very important fact to emerge from the various dipping experiments (figure 4.11) is that deposition/transfer occurs only during upstrokes and after the first upstroke the TR decreases for the subsequent ones. During the down stroke the negative values of TR indicate that the film dissolves in the subphase.

This indicates that PVDF LB films are Z-Type in nature. But the Z-Type nature gets disrupted due to the partial dissolution of PVDF into water during downstrokes. To avoid the partial dissolution of film during each downstroke the subphase was changed after deposition of one layer. For the second and subsequent layers the substrate was hung just above the surface of the water to avoid the dissolution of the already deposited film. So, the final dipping conditions are upstroke dipping speed 2 mm/min and downstroke dipping speed 15 mm/min, barrier speed 20 mm/min for dipping of Langmuir-Blodgett PVDF thin films.

In this manner 1, 3, and 8 layers were transferred. And the same were annealed for the final phase formation. The PVDF thin films deposited on glass substrate are annealed at 145°C for 4 hours and then are preserved under vacuum.

#### 4.5 Topography Analysis

The PVDF LB films formed with transfer of 1, 3, and 8 layers were characterized topographically after the  $\beta$ -phase formation using AFM

The analysis of the AFM images (figure 4.12, table 4.8) of the films clearly shows that the films are rough in nature and become more so progressively as the number of layers increases. The scan of the area between the large crystallites for 1 layer sample (figure 4.12(b)) shows that this area is very smooth with r.m.s roughness of  $\sim 6$  nm.

**Table 4.8:** Roughness analysis of the AFM images

Layers Transferred	r.m.s. Roughness (nm)
1	33
3	53
8	69

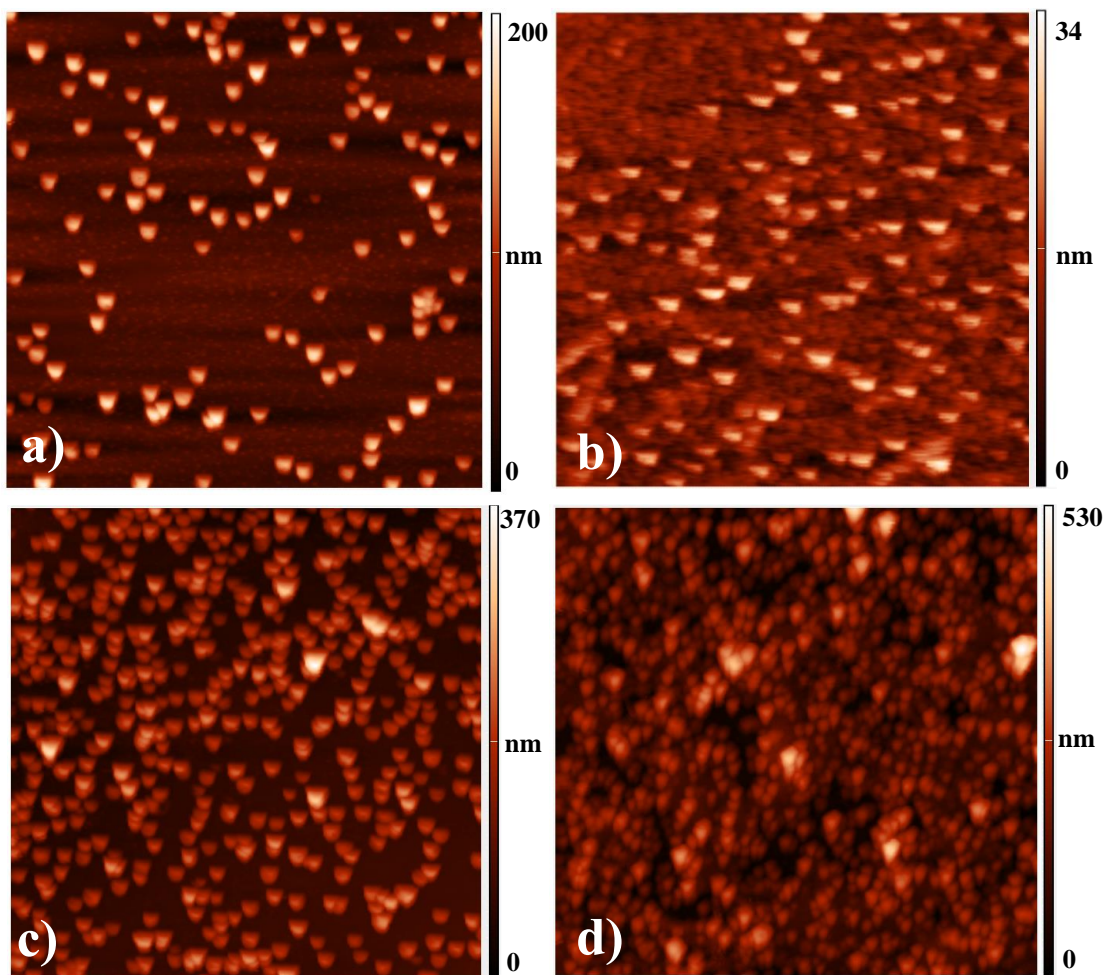


**Figure 4.12:** AFM images of PVDF Langmuir-Blodgett films on glass substrate.  $15\ \mu\text{m} \times 15\ \mu\text{m}$  AFM images of a) 1 layer c) 3 layer d) 8 layer film. b)  $3\ \mu\text{m} \times 3\ \mu\text{m}$ , image of 1 layer film in the smoother region.

#### 4.6 References

1. Xiaolin Li. et al., *Nature nanotechnology*, 3 (2008) 538-542.

---

## **Chapter 5**

### **Conclusion and future scope**

#### **5.1 Conclusion**

In the present work, the PVDF thin films are prepared by Langmuir-Blodgett deposition method with NMP solvent. To obtain good transfer characteristics the PVDF Langmuir layers were characterized for different spreading solution concentration and compression rates at 18 °C. The isotherm, hysteresis and barrier oscillation experiments show that the most stable PVDF films were obtained for spreading solution molarity of 0.0936 mol/l and 20 mm/min compression rate. These trough parameters were used for the deposition of the PVDF LB films. The role of spreading solution molarity in sharply determining the MMA and elasticity of the monolayer indicates that the initial interaction of the PVDF with the solvent (NMP) plays an important role in determining the spreading solution characteristics. A good TR is obtained for the first upstroke at 2 mm/min speed for the glass substrate. But downstrokes result in dissolution of the deposited films and also TR is reduced in the subsequent upstrokes. This indicates that Z-type nature of the PVDF LB films which is getting disrupted due to the partial dissolution of PVDF into water during downstrokes. To avoid this every single layer deposition was followed by sub-phase change. Multilayer transparent films of PVDF were synthesized by deposition of 1, 3 and 8 layers on the followed by drying and annealing. The topographic analysis of the final films shows the emergence of few large crystallites which makes the films rough.

#### **5.2 Future scope**

The effect of solvent on the monolayer and LB film characteristics need to be studied further using different aprotic solvent as well as protic solvents.









